Available online at www.sciencedirect.com
ScienceDirect
Trans. Nonferrous Met. Soc. China 21(2011) 1193−1198
Transactions of Nonferrous Metals Society of China
www.tnmsc.cn

Microstructural effects in corrosion of aluminium tube alloys

WANG Guan[1], JIAO Hui-sheng[2]

1. Institute of Mechatronics, Guangdong University of Technology, Guangzhou 510006, China;
2. Oxford Instruments (Shanghai) Ltd, Shanghai 201109, China

Received 16 August 2010; accepted 17 November 2010

Abstract: Fine gauge extruded aluminium alloy tubes can experience preferential corrosion and early failure when they are formed into "u-bend" via cold deformation. The relationship between the electrochemical reactivity and the microstructure of the bent vs straight parts of the tube was established. Investigations were carried out on two alloys containing 0.08% and 0.22% (mass fraction) of manganese. The corrosion morphology of bent tubes after immersion in salt water acetic acid test (SWAAT) solution showed the highest attack at the bent region of the high-Mn alloy. SEM characterisation of the alloys showed that each alloy has one main type of coarse intermetallic particle. However, TEM observation showed that there is a distinct difference in particle morphology between the bent and straight regions of the high-Mn tubes, the bent region revealed an additional population of 10−50 nm Mn-rich intermetallic particles, which increased both the anodic and cathodic reactivity. For the low-Mn alloy, no such effects were observed. The results suggested that cold deformation of the high-Mn tube allowed room temperature precipitation of fine Mn-rich particles, which increased the cathodic reactivity of that region by providing more cathodic sites, and increased the susceptibility to pitting by removing noble Mn from solid solution. Such an effect was not observed for the low-Mn alloy.
Key words: cold deformation; Mn precipitation; aluminium tube alloy

1 Introduction

Aluminium alloys are extensively employed as heat transfer tube materials in heat exchangers. Previous work [1−3] focused on the corrosion behaviour of tube materials in brazed heat exchangers, but very little attention was devoted to corrosion of the round tubes in mechanically expanded heat exchangers. In industrial field, it was found that some aluminium tube alloys can experience early failure in bent region, so it is valuable to give the explanation of this phenomenon.

Al-3xxx wrought alloys are widely used for architectural applications, cooking utensils, bodies of beverage cans, packaging, chemical equipment, pressure vessels, and heat exchangers [4−5]. However, it is known that the electrochemical properties are strongly influenced by different intermetallic particles. The particles increase cathodic activity of the surface and act as pit initiation sites [6−7]. It is also thought that precipitation causes solute depletion of the matrix [8]. Mn is a beneficial element. The beneficial role of Mn in Al-Mn alloys is interpreted as reducing the difference in electrochemical potential between the matrix and the intermetallic particles due to supersaturation of Mn in the matrix and Mn enrichment of the intermetallic particles [9−10].

Deformation is likely to have two effects on the electrochemical behaviour of aluminium alloys. One effect is to cause the precipitation of particles that act as local cathodes and pit initiation sites. The other effect is that the formation of precipitates will deplete the adjacent matrix in solute, making it more susceptible to dissolution [11−13].

This investigation focused on the electrochemical characterisation of the bent regions of two different aluminium tube alloys in order to establish the relationship between the microstructure associated with the regions of the tube alloys and their electrochemical behaviour.

2 Experimental

Two commercially available aluminium alloys were used in this study. The chemical compositions are given in Table 1. The alloys were supplied in the form of extruded tubes that were mechanically bent without prior or subsequent heat treatment. The microstructure of the

Corresponding author: WANG Guan; Tel: +86-20-39322367; Fax: +86-20-39322413; E-mail: GXW290@gmail.com
DOI: 10.1016/S1003-6326(11)60842-X

Table 1 Chemical composition of tube materials (mass fraction, %)

Alloy	Si	Fe	Cu	Mn	Zn	Al
Low Mn	0.04	0.18	0.005	0.08	0.18	Bal.
High Mn	0.06	0.12	0.008	0.22	0.24	Bal.

outer part of the bent region was compared with that of the straight region for each alloy via SEM (JEOL 6300) and TEM (Philips Tecnai F20). The chemical analysis of the particles was performed using EDX.

The electrochemical properties of the straight and bent regions of the tubes were investigated with immersion tests and via localised microelectrochemical measurements (Solartron Model 1285). For the immersion test, the samples were examined in the unpolished state. The specimens were immersed in the salt water acetic acid test (SWAAT) electrolyte (4.2% synthetic seawater [1], pH=2.8−3.0) for 2 d. The microelectrochemical test was performed with the tip of a pipette (diameter of 1 mm) using naturally-aerated 3.5% (0.6 mol/L) NaCl solution on samples that had been polished using 4000 grit SiC papers.

3 Results

Figure 1 shows the corrosion morphologies of the tube materials after immersion in SWAAT solution at pH=3 for 2 d. It is evident that the bent region of the high-Mn tube shows the greatest pitting attack compared with the straight region. This effect is not observed for low-Mn tube. Pits are observed to initiate at intermetallics particles, and display crystallographic facets.

The anodic and cathodic reactivities of the samples measured with the microelectrochemical cell are shown in Figs. 2 and 3. Figure 2(a) shows the anodic polarisation curves for the bent and straight regions of the high-Mn tube. In all cases, a clearly-defined breakdown potential can be observed. Figure 2(b) summarises the breakdown potentials (defined as the potential where the current density reaches 10 $\mu A/cm^2$) for both alloys. It is clear that the breakdown potential of straight region of the high-Mn alloy is higher than that of the bent region. The breakdown potentials of bent and straight regions of the low-Mn tube are the same as those of the bent high-Mn tube. However, the straight region of the high-Mn tube has a higher breakdown potential than the straight or bent region of the low-Mn tube.

Figure 3(a) shows the cathodic polarisation curves for the high-Mn tube. Figure 3(b) provides a summary of the magnitude of the cathodic current density at –1.1 V (vs SCE) for both tube alloys. The cathodic current density of the bent region of the high-Mn tube is higher than that of the straight region, and also higher than those of both the straight and bent regions of the low Mn tube.

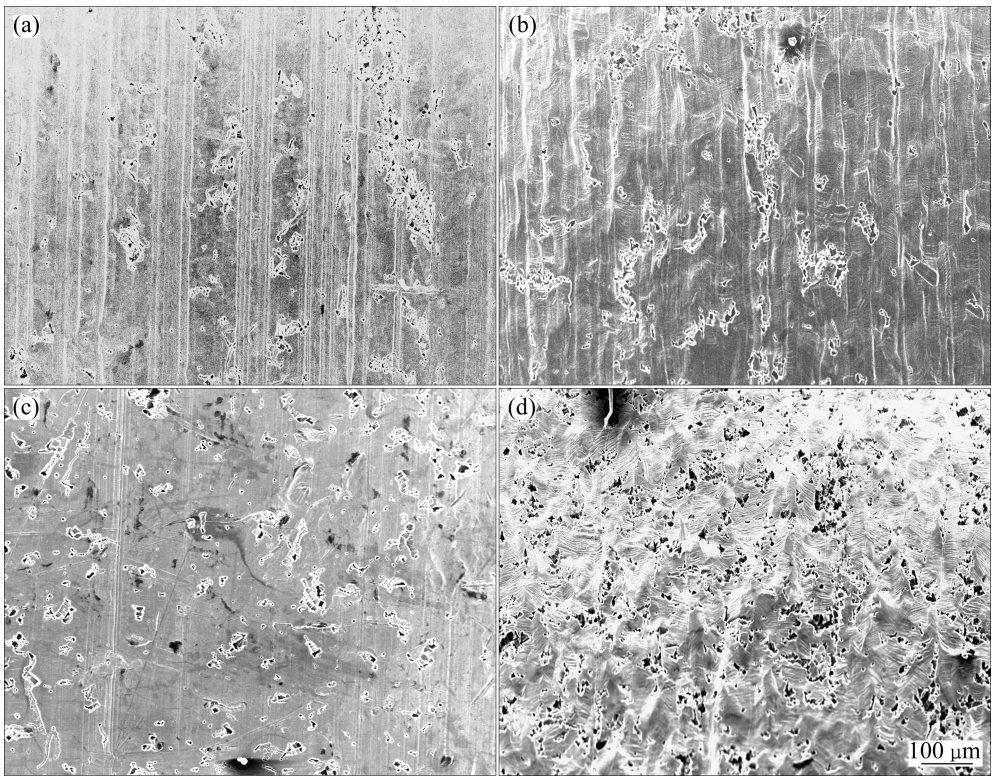

Fig. 1 Corrosion morphologies of tube materials after immersion in SWAAT solution at pH=3 for 2 d: (a) Straight region of low-Mn tube; (b) Bent region of low-Mn tube; (c) Straight region of high-Mn tube; (d) Bent region of high-Mn tube

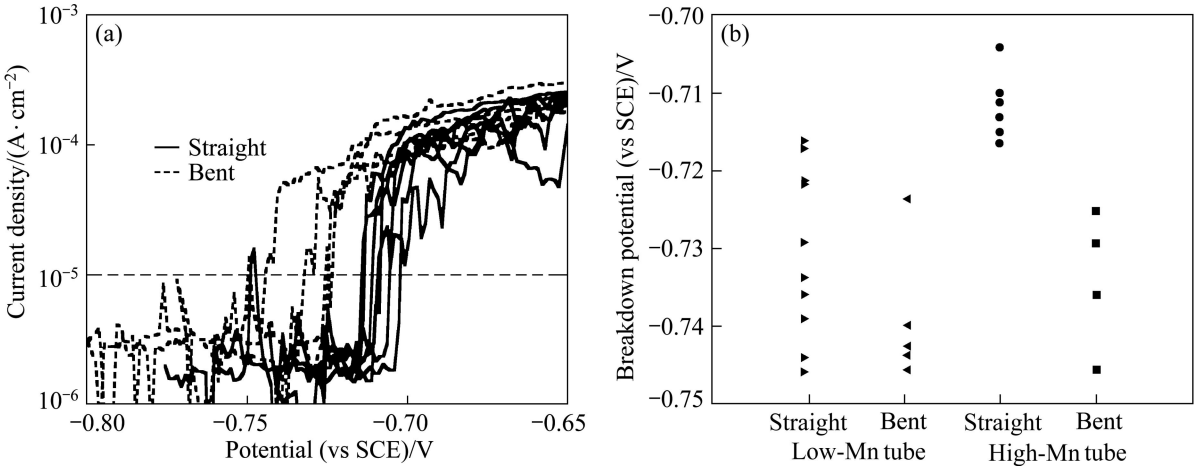

Fig. 2 Anodic polarisation curves for tube alloys in aerated 3.5% NaCl solution using microelectrochemical cell: (a) Bent and straight regions of high-Mn tube; (b) Summary of distribution of breakdown potentials determined at 10 μA/cm^2

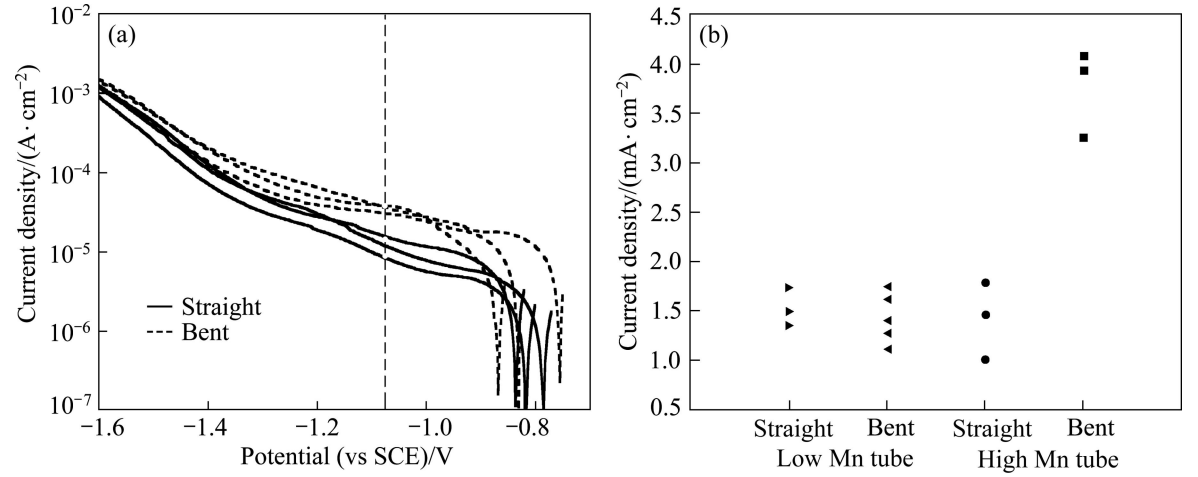

Fig. 3 Cathodic polarisation curves for tube alloys in naturally-aerated 3.5% NaCl solution using microelectrochemical cell: (a) Bent and straight regions of high-Mn tube; (b) Summary of cathodic current density at −1.1V (vs SCE)

The intermetallic particles present in all of the samples were analyzed by SEM/EDX. Figure 4 shows the SEM microstructures of the straight regions of both the alloy tubes. The bent regions appear similar at this magnification. The micron-sized particles in the low Mn tube were found to contain Al, Fe, Si and Zn, whereas those in the high-Mn tube contained Al, Mn, Fe, Si and Zn. There was no difference in the distribution of micron-sized particles between the bent and straight regions of either tube.

TEM samples were prepared from several different tubes of the two alloys. In the bright field images of both tubes, in addition to micron-sized particles that were observed using SEM, fine particles, typically <100 nm were observed. There is no difference in the number of intermetallic particles observed for the straight and bent regions of the low Mn tubes. However, for the high Mn tubes, there are more fine (<100 nm) precipitates in the bent regions than in the straight regions (Fig. 5). For each alloy, the composition of the fine particles determined from EDX on TEM is the same as that determined from SEM/EDX analysis of the micron-sized particles [5].

4 Discussion

Microstructural analysis reveals that the straight and bent regions of the low-Mn alloy contain the same Al-Fe-Si-Zn particles. The straight and bent regions of the high-Mn alloys contain Al-Fe-Mn-Si-Zn particles. However, the bent region of the high Mn alloy contains additional fine particles with a typical size <100 nm. The exact composition could not be determined, but is consistent with the composition of $Al_{12}(Fe, Mn)_3Si$ found by ZAMIN [10] in a Al-Fe-Mn-Si alloy.

The TEM results indicate that mechanical bending without subsequent heat treatment [14] causes the

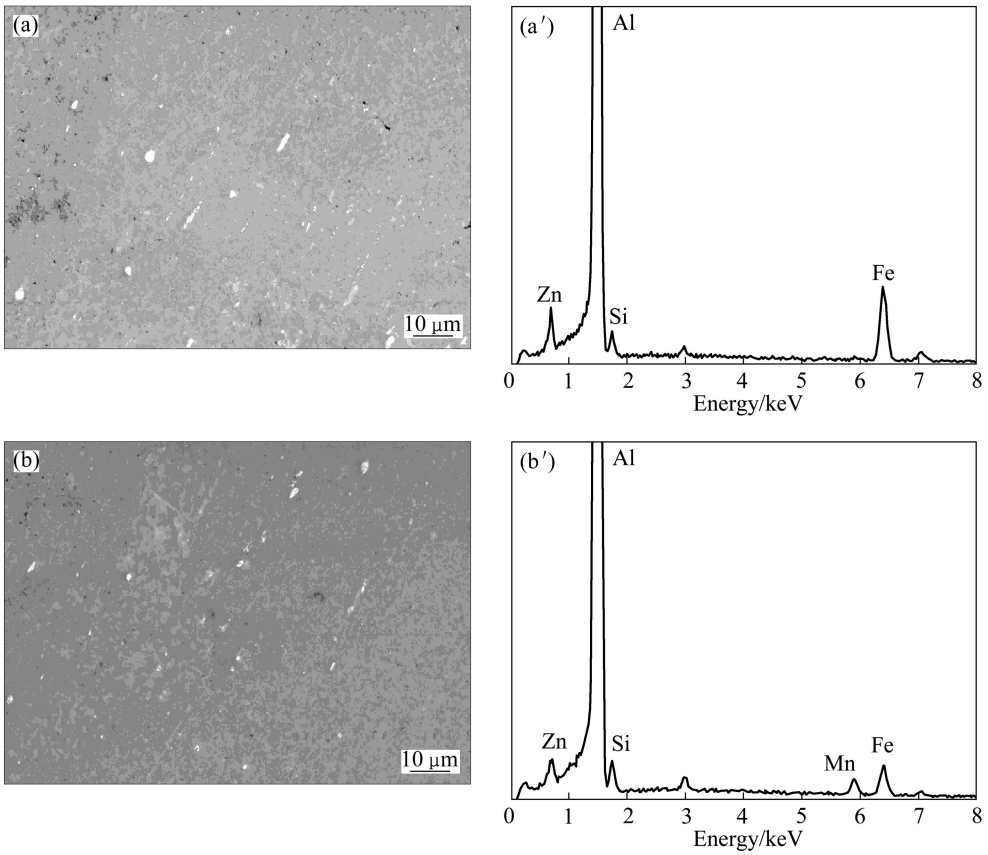

Fig. 4 SEM images and corresponding EDX element spectra for straight region of tube alloys (surface polished to 1 μm): (a), (a′) Low-Mn tube; (b), (b′) High-Mn tube

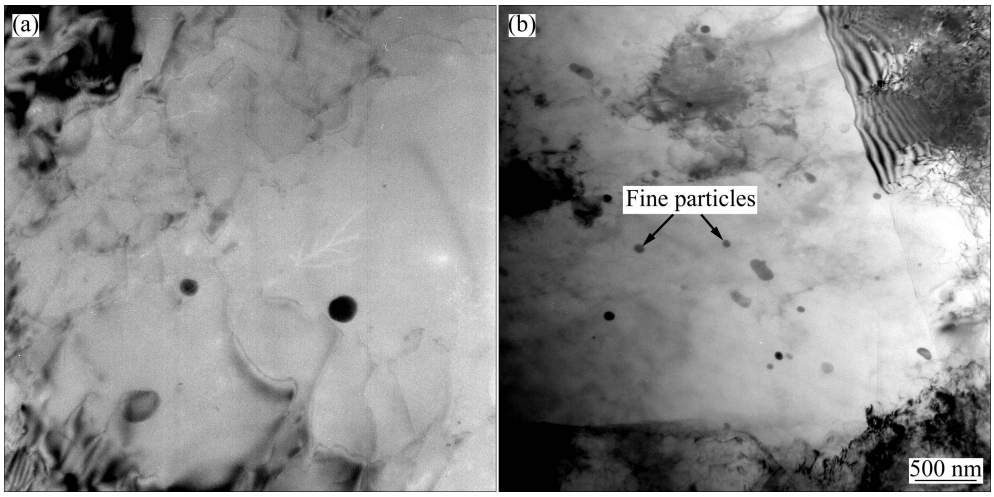

Fig. 5 TEM images of straight region (a) and bent region (b) of high-Mn tube

precipitation of Mn-containing intermetallic particles shown in Fig. 4(b). This is a surprising observation, as it would be expected that both deformation and heat treatment would be needed for particle nucleation. The presence of a high dislocation density both offers an increase in nucleation sites and enhances the diffusion coefficient of solutes. Previous studies [15−16] on the effect of plastic deformation on the precipitation kinetics of Mn-bearing phases $Al_{12}(Fe, Mn)_3Si$ and $(Mn, Fe)Al_6$ indicated that deformation reduces the temperatures at which precipitation starts, and may increase the rate of precipitation at given temperature of 300 °C by orders of magnitude [8].

Deformation alone would not normally be expected to be sufficient to allow nucleation and growth of Mn-containing particles since the diffusion rate of Mn is

slow. CHEN et al [17] observed that Mn segregation at dislocations occurred during cold rolling. They suggested that deformation increases the dislocation density, which increases both the nucleation site density and diffusivities of precipitate-forming elements in the material. Furthermore, the nucleation barrier for dislocations is much lower than that for homogenous nucleation. In addition, the solute atmosphere around dislocations enhances the rate of precipitation via an increase in the local chemical driving force.

The relationship between the deformation of the aluminium tube alloys and corrosion susceptibility was investigated using two methods: potentiodynamic measurements and immersion tests. It was found that the bent region of the high Mn tube is more susceptible to pitting corrosion (Fig. 1), has a lower breakdown potential than the straight region of the same alloy (Fig. 2) and has the highest cathodic reactivity (Fig. 3). These observations can be linked to the precipitation of fine Mn-rich particles in the bent region of the high-Mn tube.

The cathodic reactivity of aluminium alloys is determined by the presence of intermetallic particles [10−11]. Thus, the increase in the presence of precipitates is likely to cause an increase in the cathodic reactivity as observed here. Precipitates are also known to be pit initiation sites in aluminium alloys [18−19]. This correlates with the increased anodic reactivity (lower breakdown potential). The increase in anodic reactivity is also likely to be influenced by the loss of Mn from solid solution, which has also been observed to be beneficial in decreasing the dissolution rate of aluminium alloys [9−10].

The beneficial effect of Mn in solid solution is highlighted by the observation that the corrosion behaviour of the low Mn alloy is similar to that of the bent region of the high Mn alloy after precipitation of Mn-rich particles.

The above results indicate the role of deformation and effect of Mn in solid solution on the corrosion behaviour of aluminium tube alloys. No previous work has been done on the cold deformation effect on corrosion behaviour of the Al-Fe-Mn-Si-Zn system. The present work has highlighted the cold deformation effects of enhanced precipitation in increasing both anodic and cathodic reactivities of the bent region of aluminium tube alloys.

5 Conclusions

1) There are more fine (<100 nm) Mn-rich particles in the bent region of high-Mn tube than in the straight region of high-Mn tube, but there is no difference between the straight and bent regions of low-Mn tube.

2) The straight region of high-Mn tube has lower anodic reactivity than that of the low-Mn tube. This may be due to the presence of Mn in solid solution, which is known to improve corrosion resistance.

3) The bent region of high-Mn tube has higher anodic reactivity than the straight region. This may be due to the loss of Mn from solid solution as a result of precipitation.

4) The bent region of high-Mn tube has a higher cathodic reactivity than the straight region. This is probably a result of the increase in the number of cathodically active particles.

References

[1] STEVEN M. Corrosion of aluminium brazing sheet [D]. Netherland: University of Delft, 2002.

[2] WOODS R A, SCOTT A C, HARRIS J F. A corrosion-resistance alloy for vaccum-brazed aluminum heat exchangers [J]. SAE Technical Paper, 1991, 910591: 655−658.

[3] LIJIMA K, HAGIWARA M, MIURA T, BABA Y, TANABE Z, HASEGAWA Y. Development of new aluminum alloy sheets for sacrificial anode [J]. SAE Technical Paper, 1986, 860080: 135−137.

[4] POLMEAR I J. Light alloys—Metallurgy of the light metals [M]. London: Arnold, 1995: 24−26.

[5] MONDOLFO L F. Aluminum alloys structure and properties [M]. London: Butterworths, 1976.

[6] WANG G. Heat treatment effect on the corrosion of aluminium heat exchanger fin materials [J]. Corrosion Science and Protection Technology, 2010, 22(3): 180−183. (in Chinese)

[7] AMBAT R, DAVENPORT A J, SCAMANS G M, AFSETH A. Effect of iron-containing intermetallic particles on the corrosion behaviour of aluminium [J]. Corrosion Science, 2006, 48(11): 3455−3471.

[8] AMBAT R, DAVENPORT A J, AFSETH A, SCAMANS G. Electrochemical behavior of the active surface layer on rolled aluminum alloy sheet [J]. J Electrochem Soc B, 2005, 151(1): 53−58.

[9] NISANCIOGLU K, LUNDER O. Significance of the electrochemistry of Al-base intermetallics in determining the corrosion behaviour of aluminium alloys[C]//STARKE E A, SANDERS T H, CASSADA W A. Aluminum Alloys—Their Physical and Mechanical Properties. Charlottesville: Engineering Materials Advisory Services Ltd, 1986: 111−126.

[10] ZAMIN M. The role of Mn in the corrosion behavior of Al-Mn alloys [J]. Corrosion, 1981, 37(8): 627−632.

[11] NISANCIOGLU K. Electrochemical behaviour of aluminium-base intermetallics containing iron [J]. J Electrochem Soc, 1990, 137(1): 69−77.

[12] PARDO A, MERINO M C, MERINO S, VIEJO F, CARBONERAS M, ARRABAL R. Influence of reinforcement proportion and matrix composition on pitting corrosion behaviour of cast aluminium matrix composites [J]. Corrosion Science, 2005, 47(7): 1750−1764.

[13] KNIGHT S P, SALAGARAS M, WYTHE A M, de CARLO F, DAVENPORT A J, TRUEMAN A R. In situ X-ray tomography of intergranular corrosion of 2024 and 7050 aluminium alloys [J]. Corrosion Science, 2010, 52(12): 3855−3860.

[14] WANG G. Microstructural effects in the corrosion of automotive aluminium heat exchangers [D]. UK: The University of Birmingham, 2007.

[15] LUIGGI N J. Isothermal precipitation of commercial 3003 Al alloys studied by thermoelectric power [J]. Metallurgical and Materials Transactions B, 1997, 28(1): 125−130.
[16] LUIGGI N J. Isothermal precipitation of commercial 3005 Al alloys studied by thermoelectric power [J]. Metallurgical and Materials Transactions B, 1997, 28(1): 149−155.
[17] CHEN S P, KUIJPERS N C W, ZWAAG S. Effect of microsegregation and dislocations on the nucleation kinetics of precipitation in aluminium alloy [J]. Materials Science and Engineering A, 2003, 341(1−2): 296−305.
[18] CECCHETTO L, AMBAT R, DAVENPORT A J, DELABOUGLISE D, PETIT J P, NEEL O. Emeraldine base as corrosion protective layer on aluminium alloy AA5182: Effect of the surface microstructure[J]. Corrosion Science, 2007, 49(2): 818−829.
[19] BAKOS I, SZABO S. Corrosion behaviour of aluminium in copper containing environment[J]. Corrosion Science, 2008, 50(1): 200−205.

显微组织对铝管腐蚀的影响

王 冠[1], 焦会胜[2]

1. 广东工业大学 机电学院，广州 510006；2. 牛津仪器(上海)有限公司，上海 201109

摘 要：发现一些管状铝合金通过机械变形弯曲成 U 形时更容易在弯曲表面发生腐蚀。建立了管状铝合金的水平和弯曲表面的显微组织与腐蚀的关系。通过对含 0.08 %及 0.22 % Mn 的两种铝合金弯管弯曲部分的显微组织的观察，及在酸性盐水(SWAAT)中的腐蚀形貌及微观电化学反应的研究，发现高 Mn 铝管在弯曲表面较易发生点蚀，有较低的击穿电压及较高的阴极电流密度。SEM 及 TEM 观察发现此现象的产生与高 Mn 铝管弯曲处弥散的粒径小于 100 nm 的富含 Mn 的合金二次相有关。

关键词：机械冷弯曲；Mn 颗粒；管状铝合金

(Edited by YUAN Sai-qian)